# Reagentless Detection of Mycobacteria tuberculosis H37Ra in Respiratory Effluents in Minutes

**ARTICLE** *in* ANALYTICAL CHEMISTRY · JULY 2008

Impact Factor: 5.64 · DOI: 10.1021/ac8002825 · Source: PubMed



**7 AUTHORS**, INCLUDING:

Kristl L Adams
Lawrence Livermore National Laboratory
**15** PUBLICATIONS **72** CITATIONS
SEE PROFILE

M.J. Bogan
Stanford University
**110** PUBLICATIONS **3,826** CITATIONS
SEE PROFILE

Audrey Martin Williams
Lawrence Livermore National Laboratory
**13** PUBLICATIONS **128** CITATIONS
SEE PROFILE

Matthias Frank
Lawrence Livermore National Laboratory
**175** PUBLICATIONS **3,981** CITATIONS
SEE PROFILE

*Anal. Chem.* **2008,** *80,* 5350–5357

# Reagentless Detection of *Mycobacteria tuberculosis* H37Ra in Respiratory Effluents in Minutes

**Kristl L. Adams,[†] Paul T. Steele,[†] Michael J. Bogan,[†] Nicole M. Sadler,[†,‡] Sue I. Martin,[†] Audrey N. Martin,[†,§] and Matthias Frank*[,†]**

*Lawrence Livermore National Laboratory, Livermore, California 94550, University of California, Davis, California 95616, and Michigan State University, East Lansing, Michigan 48824*

**Two similar mycobacteria, *Mycobacteria tuberculosis* H37Ra and *Mycobacteria smegmatis* are rapidly detected and identified within samples containing a complex background of respiratory effluents using single-particle aerosol mass spectrometry (SPAMS). *M. tuberculosis* H37Ra (TBa), an avirulent strain, is used as a surrogate for virulent tuberculosis; *M. smegmatis* (MSm) is utilized as a near-neighbor confounder for TBa. Bovine lung surfactant and human exhaled breath condensate are used as first-order surrogates for infected human lung expirations from patients with pulmonary tuberculosis. This simulated background sputum is mixed with TBa or MSm and nebulized to produce conglomerate aerosol particles, single particles that contain a bacterium embedded within a background respiratory matrix. Mass spectra of single conglomerate particles exhibit ions associated with both respiratory effluents and mycobacteria. Spectral features distinguishing TBa from MSm in pure and conglomerate particles are shown. SPAMS pattern matching alarm algorithms are able to distinguish TBa-containing particles from background matrix and MSm for >50% of the test particles, which is sufficient to enable a high probability of detection and a low false alarm rate if an adequate number of such particles are present. These results indicate the potential usefulness of SPAMS for rapid, reagentless tuberculosis screening.**

Virulent tuberculosis (TBv) was predicted to infect ~9 million people worldwide and be fatal to 1.7 million in 2007.[1] Tuberculosis typically attacks the lungs (pulmonary TBv) but can infect almost any organ of the body including the joints, bones, bone marrow, urinary tract, central nervous system, muscles, skin, and throat. TBv is an airborne contagious disease that spreads when a person with tuberculosis of the lungs or throat coughs, sneezes, or talks. It is important to distinguish between a latent tuberculosis infection and tuberculosis the disease. Inhaling airborne tubercle bacilli from the respiratory effluents of a person with TBv can infect the lungs, but with a healthy immune system, this infection may remain dormant for years without causing illness; this is referred to as a latent TBv infection. Latent infections are not contagious, though they are at risk for progression to the active tuberculosis disease, which can be spread to others.[1] Persons with HIV or AIDS and a latent TBv infection have a much higher risk of developing active TBv (~10%/year) than does the general population (~10% in a lifetime).[2] Left untreated, a person with active TBv disease will spread the infection to an average of 10−15 people every year.[3] Early detection and treatment of tuberculosis is key to controlling the spread of this deadly disease.

Current methods for diagnosing TBv include a skin test, tubercle bacilli counting in a sputum smear, culture of the bacteria, DNA amplification via PCR, and chest radiography.[4–9] Each of these methods has advantages and disadvantages, but none is suited for rapid screening of large numbers of potential patients.

Lacking a means of rapid screening, clinicians often misdiagnose tuberculosis; a retrospective four-month study conducted in an urban Los Angeles hospital emergency department showed either initial release or nonisolation of over 40% of culture-positive *Mycobacterium tuberculosis* cases.[8] The same study showed the resources wasted in unnecessary precautions taken for patients eventually found to be tuberculosis negative; for every tuberculosis-positive patient, 624 patients were screened for tuberculosis at triage, 130 chest radiographs were taken, and 22 patients were placed in isolation. In either false diagnosis scenario, there is tremendous cost. False negatives or poor tuberculosis recognition can result in releasing tuberculosis-positive patients back into the community. Nonisolation of these false negative tuberculosis patients presents a risk of disease transmission to others, and without treatment their own health may deteriorate. In correcting this misdiagnosis, healthcare facilities will (at great cost) conduct infection-control contact tracing of the released patient to administer tests and additional treatments to those that may have come in contact with the tuberculosis patient. Consequently, false

* To whom correspondence should be addressed. E-mail: frank1@llnl.gov. Phone: 925-423-5068. Fax 925-424-2778.

[†] Lawrence Livermore National Laboratory.

[‡] University of California, Davis.

[§] Michigan State University.

(1) Editorial, *Nat. Med.* **2007**, *13*, 263.

(2) Blumberg, H. M.; Leonard, M. K.; Jasmer, R. M. *JAMA, J. Am. Med. Assoc.* **2005**, *293*, 2776–2784.

(3) World Health Organization, Tuberculosis, Fact sheet 104. http://www.who.int/mediacentre/factsheets/fs104/en/, accessed March 2007.

(4) Dinnes, J.; Deeks, J.; Kunst, H.; Gibson, A.; Cummins, E.; Waugh, N.; Drobniewski, F.; Lalvani, A. *Health Technol. Assess.* **2007**, 11.

(5) Cho, S.-N.; Brennan, P. J. *Tuberculosis* **2007**, *87*, S14–S17.

(6) Kalantri, S.; Pai, M.; Pascopella, L.; Riley, L.; Reingold, A. *BMC Infect. Dis.* **2005**, *5*, 59.

(7) Perkins, M. D.; Cunningham, J. *J. Infect. Dis.* **2007**, *196*, S15–27.

(8) Sokolove, P. E.; Rossman, L.; Cohen, S. H. *Acad. Emergency Med.* **2000**, *7*, 1056–1060.

(9) Steingart, K. R.; Henry, M.; Laal, S.; Hopewell, P. C.; Ramsay, A.; Menzies, D.; Cunningham, J.; Weldingh, K.; Pai, M. *PLoS Med.* **2007**, *4*, e202.



10.1021/ac8002825 CCC: $40.75 
Published on Web 06/18/2008

negatives tend to increase the anxiety level of the public at large and the exposed healthcare workers. Alternatively, tuberculosis false positives cause a tremendous toll on resources including long unnecessary hospitalization times and higher demands on equipment and personnel. False positives may also lead to broad isolation practices, decreased patient contact, and diminished bedside manner thus resulting in suboptimal care. It is clear that a rapid tuberculosis screening technique could facilitate early detection and limit unnecessary isolation, thus providing better patient care and reducing the toll on healthcare facility resources.

A single-particle aerosol mass spectrometry (SPAMS) instrument was developed at Lawrence Livermore National Laboratory (LLNL) for rapid aerosol detection of low-concentration pathogens in the presence of high background concentrations.[10–12] The original instrument and algorithm design assumed aerosols would contain pathogen particles that are separate and distinct from background particles. A relevant scenario might involve anthrax spores released in an office environment in which case a given aerosol particle would either be a spore (~100% pathogen) or a harmless background particle (0% pathogen).[10,11] The data presented herein advance this detection capability by addressing a new type of particle, a conglomerate consisting of both pathogen and background material. In this work, a single conglomerate particle contains a simulant pathogen (TBa or MSm) embedded in respiratory background materials (lung surfactant or exhaled breath condensate). These conglomerate particles are a first-order representation of expected sputum samples obtained from persons with active pulmonary tuberculosis. SPAMS rapidly and reagentlessly identifies and differentiates these simulant pathogens embedded within respiratory background materials, highlighting the potential for rapid tuberculosis screening in a clinical setting.

## METHODS AND MATERIALS

**Sample Preparation and Aerosolization.** Six pure samples are analyzed: lung surfactant (LS), exhaled breath condensate (EBC), *M. tuberculosis* H37Ra (TBa), *Mycobacterium smegmatis* (MSm), TBa growth media, and MSm growth media. Four mixtures are analyzed: TBa+LS, MSm+LS, TBa+EBC, and MSm+EBC. All liquid suspension samples are introduced into the SPAMS system by aerosolization in a biosafety cabinet via nitrogen gas (flow rate ~1.2 L/min) using a low-volume disposable nebulizer (Salter Labs, Arvin, CA). Aerosol droplets are directed through an in-line diffusion dryer containing a silica desiccant resulting in analyzed particles with aerodynamic diameters in the range of 0.5−2.5 $\mu$m (as measured by the SPAMS instrument).

**(a) Lung Surfactant Sample.** Survanta brand bovine LS is obtained from Abbott Laboratories and diluted ~1:10 in deionized water before aerosolization.

**(b) Exhaled Breath Condensate Sample.** Breath condensate is collected from a healthy person using an R-Tube assembly (Respiratory Research Inc., Charlottesville, VA).

**(c) *M. smegmatis*, MSm+LS, and MSm+EBC Samples.** *M. smegmatis* (ATCC 19420) is grown in Middlebrook 7H9 broth (BD 271310) supplemented with 0.2% glycerol and 10% albumin−dextrose−catalase enrichment (BD 212352). Cultures are incubated at 37 °C on a platform shaker (150 rpm) until mid to late log phase and then collected by centrifugation. Water-soluble media components are removed by washing the pellet 3 times with sterile water. The washed pellet is subsequently resuspended in water to a stock concentration of $\sim 5.5 \times 10^7$ cells/mL (as measured by bacterial counting under 400× magnification) and refrigerated until SPAMS analysis. Aliquots of the prepared MSm are analyzed within hours of the postculturing treatment. All MSm-containing samples (MSm, MSm+LS, MSm+EBC) are diluted 1:3 in water, LS, or EBC, respectively, for a final concentration of $\sim 1.8 \times 10^7$ MSm cells/mL.

**(d) *M. tuberculosis*, TBa+LS, and TBa+EBC Samples.** *M. tuberculosis* H37Ra (ATCC 25177) is grown in Dubos broth base (Difco) supplemented with 10% Dubos medium bovine albumin (Difco), 5% glycerol, and 0.25% Tween 80. Cultures are incubated on a platform shaker (150 rpm) at 37 °C in vented culture flasks until mid to late log phase and then collected by centrifugation. Clumping is minimized by occasional gentle vortexing. Water-soluble media components are removed by washing the pellet 3 times with sterile water. The washed pellet is subsequently resuspended in water to a stock concentration of $\sim 9 \times 10^7$ cells/mL (as measured by bacterial counting under 400× magnification) and refrigerated until SPAMS analysis. Aliquots of the prepared TBa are analyzed within hours of the postculturing treatment. All TBa-containing samples (TBa, TBa+LS, TBa+EBC) are diluted 1:3 in water, LS, or EBC, respectively, for a final concentration of $\sim 3 \times 10^7$ TBa cells/mL.

**SPAMS Instrumentation.** Experiments are performed on a SPAMS system with a reflectron time-of-flight configuration described in detail elsewhere.[13–17] Particles sampled through the SPAMS inlet are passed through five successive instrument regions: focusing, tracking/sizing, charge, fluorescence, and dual polarity mass spectrometer; see Figure 1. Particles within the respirable size range (~1−10 $\mu$m) are focused by an aerodynamic lens stack into a collimated, vertically orientated beam. The lens stack accelerates every particle to a velocity dependent on its aerodynamic diameter; small particles travel faster than larger particles. Particles cross three or more CW laser beams in the tracking and sizing region, and the resultant scattered light is detected by separate channel photomultiplier tubes. The scattered light timing determines the particle's position, velocity, and, with proper calibration, aerodynamic diameter. The position and velocity are then used to trigger subsequent stages of the instrument.


(10) Srivastava, A.; Pitesky, M. E.; Steele, P. T.; Tobias, H. J.; Fergenson, D. P.; Horn, J. M.; Russell, S. C.; Czerwieniec, G. A.; Lebrilla, C. S.; Gard, E. E.; Frank, M. *Anal. Chem.* **2005**, *77*, 3315–3323.

(11) Tobias, H. J.; Pitesky, M. E.; Fergenson, D. P.; Steele, P. T.; Horn, J.; Frank, M.; Gard, E. E. *J. Microbiol. Methods* **2006**, *67*, 56–63.

(12) Tobias, H. J.; Schafer, M. P.; Pitesky, M.; Fergenson, D. P.; Horn, J.; Frank, M.; Gard, E. E. *Appl. Environ. Microbiol.* **2005**, *71*, 6086–6095.

(13) Gard, E.; Mayer, J. E.; Morrical, B. D.; Dienes, T.; Fergenson, D. P.; Prather, K. A. *Anal. Chem.* **1997**, *69*, 4083–4091.

(14) Fergenson, D. P.; Pitesky, M. E.; Tobias, H. J.; Steele, P. T.; Czerwieniec, G. A.; Russell, S. C.; Lebrilla, C. B.; Horn, J. M.; Coffee, K. R.; Srivastava, A.; Pillai, S. P.; Shih, M. T. P.; Hall, H. L.; Ramponi, A. J.; Chang, J. T.; Langlois, R. G.; Estacio, P. L.; Hadley, R. T.; Frank, M.; Gard, E. E. *Anal. Chem.* **2004**, *76*, 373–378.

(15) Russell, S. C.; Czerwieniec, G.; Lebrilla, C.; Tobias, H.; Fergenson, D. P.; Steele, P.; Pitesky, M.; Horn, J.; Srivastava, A.; Frank, M.; Gard, E. E. *J. Am. Soc. Mass. Spectrom.* **2004**, *15*, 900–909.

(16) Steele, P. T.; Tobias, H. J.; Fergenson, D. P.; Pitesky, M. E.; Horn, J. M.; Czerwieniec, G. A.; Russell, S. C.; Lebrilla, C. B.; Gard, E. E.; Frank, M. *Anal. Chem.* **2003**, *75*, 5480–5487.

(17) Coffee, K. R.; Riot, V. J.; Farquar, G.; Steel, P.; Woods, B. W.; Benner, W. H.; Rohner, U.; Fergenson, D. P.; Tobias, H. J.; Frank, M. E. G. Unpublished work, LLNL, 2006.

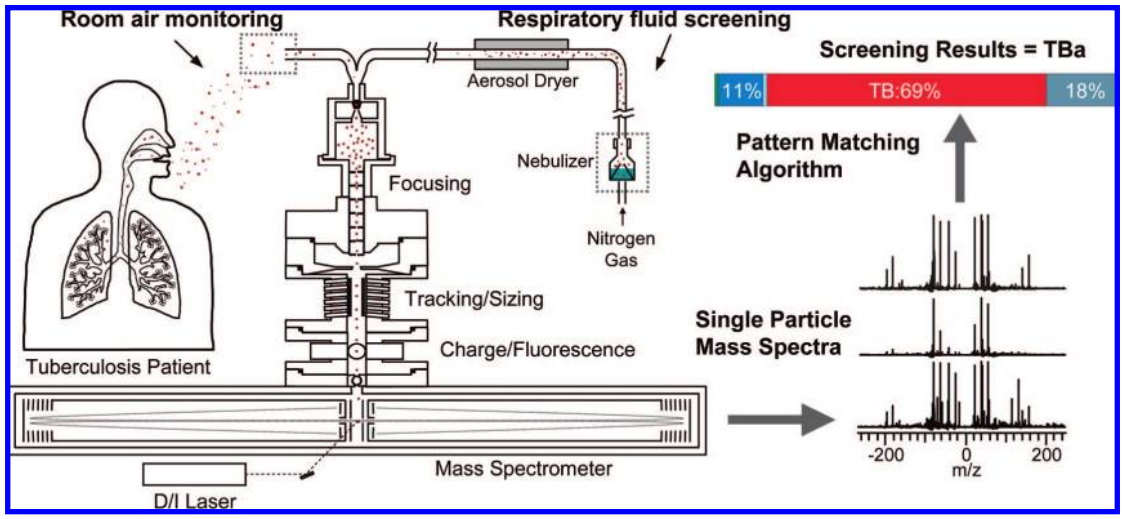


**Figure 1.** Proposed SPAMS deployment in a clinical environment for rapid tuberculosis screening. Two sampling methods are depicted: general room air monitoring and direct sampling of aerosolized respiratory effluent samples. The SPAMS instrument used for the experiments here consists of five regions: particle focusing, tracking/sizing, charge analysis, fluorescence analysis, and dual polarity laser desorption/ionization (D/I) mass spectrometry. Single-particle data are processed with a pattern matching algorithm and tuberculosis screening results are obtained in minutes.

After the sizing and tracking stage, particles pass successively through charge and fluorescence stages where particle charge and laser-induced fluorescence properties are measured. In situations with high background particle concentrations, the charge and fluorescence stages may be used for preselection to identify particles of interest for selective analysis by the mass spectrometer. Data from these stages are not utilized in the analysis for the experiments described here.

The mass spectrometer stage fires a Q-switched desorption/ionization (DI) laser emitting 266-nm wavelength pulses of ~6-ns duration. External optics produce a roughly flat-topped laser beam profile with a diameter of ~400 $\mu$m in the ionization region in the center of the mass spectrometer.[18] Spectra are acquired with a laser pulse energy of ~0.95 mJ resulting in a fluence of ~0.76 J/cm$^2$.[16] For each individual particle, positive and negative ions are created by the D/I laser. Ions of each polarity are extracted in opposite directions by two opposing reflectron time-of-flight mass spectrometers. Thus, for each particle, a complete $m/z$ spectrum is obtained in both ion polarities. Approximately 800−1000 bipolar mass spectra were obtained for each sample.

In general, data from each measurement channel is correlated for each individual particle and processed for particle-type identification. A training set of data is used to build an alarm library of particle types, which is run against independent test sets of data to identify individual particles and ultimately determine particle identification rates. The SPAMS instrument and software algorithms can be used for real-time active detection and alarming once an alarm library is made.[19,20] In these first experiments, an appropriate alarm library must be built; therefore, training and test data were acquired simultaneously and postanalyzed to determine identification rates for the test set. Alarm results described in this paper are based solely on mass spectral patterns, though particle size, charge, and fluorescence could be selectively utilized.

**Particle Identification.** The ions generated in each polarity are ultimately detected with microchannel plates producing an electrical current proportional to the incident ion flux. The resulting voltage is digitized at 500 MHz using an 8-bit digitizer (Signatec, PDA 1000). In each polarity, 32 768 ($2^{15}$) data points are acquired encompassing flight times from ~0 to 65 $\mu$s or masses of 1 to >1200 Da for singly charged ions. Calibration and baseline correction are performed on the raw spectral data producing a bipolar calibrated spectrum for each particle. Next, a vector representation of the corrected data in each polarity is produced, where the $n$th element of the vector holds the maximum value of the data falling between mass-to-charge ratios $n-0.5$ and $n+0.5$. Assuming a properly calibrated spectrum, the vector representation holds the maximum height of every ion peak versus its mass-to-charge ratio rounded to the nearest whole number. A separate vector is formed for each polarity for each analyzed particle. It should be noted that this is distinct from earlier work where the vector elements generally held peak areas rather than peak heights.[14,20] Height was used here because is enabled better differentiation of the studied particles.

The alarm library is formed as follows. Individual particles for each sample are clustered based on spectral similarity or more specifically the angle between the vector representations of their mass spectra. Clusters generated by and characteristic of the particle type of interest are preferentially retained. Small clusters containing atypical spectra or spectra resulting from impurities or contaminants in the sample are discarded. For example, 88% of the single-particle spectra produced by the pure TBa sample were retained as good clusters; most discarded clusters showed spectra characteristic of salt particles. A representative spectrum from each retained cluster is stored in the alarm library for comparison to unknown particle spectra. Consequently, the

(18) Steele, P. T.; Srivastava, A.; Pitesky, M. E.; Fergenson, D. P.; Tobias, H. J.; Gard, E. E.; Frank, M. *Anal. Chem.* **2005**, *77*, 7448–7454.
(19) Riot, V.; Coffee, K.; Gard, E.; Fergenson, D.; Ramani, S.; Steele, P. DSP-Based Dual-Polarity Mass Spectrum Pattern Recognition for Bio-Dection; Sensor Array and Multichannel Signal Processing, IEEE Workshop, 2006; pp 98−101.
(20) Steele, P. T.; Farquar, G. R.; Martin, A. N.; Coffee, K. R.; Riot, V. J.; Martin, S. I.; Fergenson, D. P.; Gard, E. E.; Frank, M. *Anal. Chem.* In press.

library contains multiple representative spectra for each particle type.

As has been described elsewhere,[14,19,20] the overall ion pattern is identified by comparison to an alarm library of known spectral types in a process generally referred to as pattern matching. The basic metric of similarity is the angle between vectors, which is calculated after vector elements representing certain large and ubiquitous ion peaks have been set to zero, thus allowing distinguishing features with smaller amplitudes to contribute. In the present case, vector elements representing $m/z$ values of +1:5, +22:24, +38:40, −1:5, −25:27, −41:43, and −79 were excluded because they arise from very common ions (e.g., $Na^+$, $K^+$, $CN^-$, $CNO^-$, and $PO_2^-$) that are of little value in discriminating simulants from backgrounds. Further refinements in the identifications can be made using rules trees, but this approach was not utilized here.

Finite misidentification rates are common for single-particle analysis and may even be significant in some cases. However, the rate of overall sample misdiagnosis does not raise in conjunction with single-particle misidentification rates. Just as the probability of flipping a coin 10 times and getting 10 tails is lower than the probability of flipping a coin once and getting a tail, the probability of misidentifying a given particle type repeatedly is much lower than the probability of misidentifying it once. Thus, multiple particles must be identified as TBa, for example, before a positive TBa detection is claimed. More precisely, a positive diagnosis will only result when the number of particles identified as a particular threat type exceeds an alarm threshold set specifically for that threat. The exact threshold value is determined with statistical equations that take into account real-time estimates of interfering particle concentrations and their previously measured misidentification rates. A higher alarm threshold provides a lower false positive rate, but some loss of sensitivity and thus a higher false negative rate will result. Nonetheless, given an efficient and rapid instrument with sufficient sample, low false positive and negative rates can be obtained simultaneously even with significant single-particle misidentification. Furthermore, the tradeoff between false positive and false negative rates can be optimized or adjusted to suite user preference so long as the correct and incorrect single-particle identification rates are known for relevant particle types.

## RESULTS AND DISCUSSION

The proposed scenario, shown in Figure 1 and discussed in detail later, provides a sketch of the experiments described herein: simulated patient respiratory effluent containing TBa is aerosolized into the SPAMS instrument, spectra of conglomerate particles are individually compared to a pattern matching library, and an accurate diagnosis is potentially obtained in minutes.

**Analysis of Single-Component Aerosols.** A modest 50-particle average mass spectral comparison, seen in Figure 2, reveals clear differences in TBa, MSm, LS, and media spectra. Pure EBC did not readily produce spectra and is thus not shown; this was expected for EBC, as it is primarily water and produces <1-$\mu$m-diameter particles that are not efficiently analyzed. In pure samples, averaging minimizes the impact of shot-to-shot variations, increases signal-to-noise ratios, and allows for identification of important mass spectral features. Thus, averages will be shown in most figures in this paper for clarity and ease of visualization although single-particle mass spectra were used for pattern

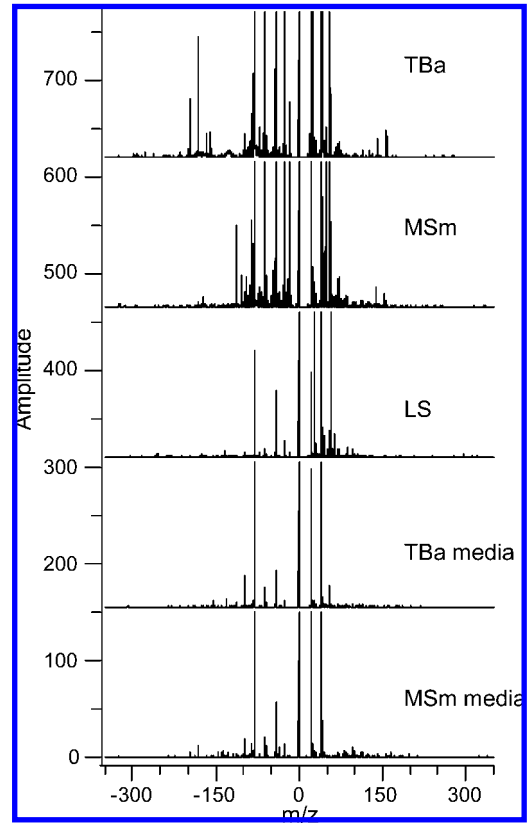


**Figure 2.** Bipolar mass spectra from pure samples of *M. tuberculosis* H37Ra (TBa), *M. smegmatis* (MSm), lung surfactant (LS), TBa growth media, and MSm growth media. The plotted mass range is limited to ±350 mass-to-charge units to emphasize the largest ion signals, though smaller peaks were evident out to ±500 *m/z* units. Each spectrum is an average of 50 individual single-particle spectra and the amplitude of the offset spectra is clipped at 150 to enhance the visibility of lower amplitude signals.

matching and particle identification. Averages are also used to evaluate peak identities in the conglomerate sample data sets. For example, pure media and bacteria mass spectra were compared to discover possible media contributions to the ion signal in bacteria-containing samples. These shared mass spectral peaks may occur from either media contamination or similar sample chemistries; such peaks are marked with an asterisk (*) in all figures and text. In real-world applications, averaging reduces instrument sensitivity since background particles are unavoidably averaged together with spectra from particles of interest. Single-spectrum analysis must therefore be investigated and herein lays the strength of SPAMS. Individual spectrum analysis, with no averaging, has distinct advantages including rapid, near real-time analysis and straightforward elimination of background particles. Nonetheless, a major challenge in realizing a SPAMS-based tuberculosis screening tool is the shot-to-shot consistency of single mass spectra obtained from individual particles. Particle position in the D/I laser spot is partially responsible for this variation,[18] but biological samples have additional natural variations in structure and chemical composition that further increase the spectral variations.

To address shot-to-shot variability, we first investigate the variability of TBa single-particle bipolar mass spectra. Four single-shot mass spectra for pure TBa, shown in Figure 3, are representative of different TBa spectral types and depict in part the

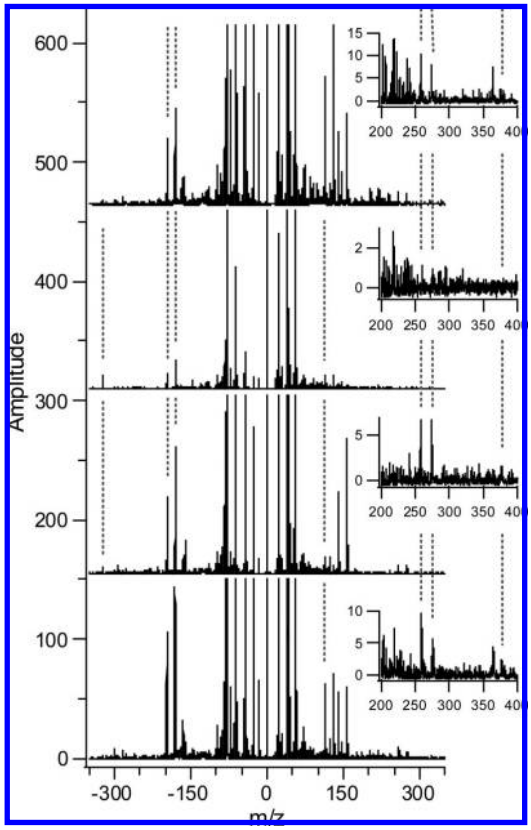


**Figure 3.** Four single-particle bipolar mass spectra of individual *M. tuberculosis* H37Ra. Insets show ions detected in the *m*/*z* range 200−400. Guidelines are inserted to highlight a few consistent peaks; however, pattern persistence can be seen in excess of guiding lines. The two most persistent ions associated with TBa are $m/z = -197$ and −181. Spectral amplitude is limited to 150 to reveal low-amplitude peaks.

breadth of variation often encountered in single-cell analysis. Even with these broad variations, some persistent ion peaks are evident. Although a single spectrum may not contain all peaks indicative of TBa, it will likely contain some characteristic peaks. An alarm algorithm may be based solely on the recognition of a small number of specific mass spectral peaks, but expected particle-to-particle variations in the ion pattern may easily confound this type of approach. For this reason, the identification method used in this experiment is not based on a single peak recognition or even on a single spectral pattern. Rather, identification is based on full-spectrum pattern matching to a library of multiple spectral types for each particle class (TBa, MSm, LS, media, etc.). Training on realistic samples forces the library to encompass expected natural variations, thus strengthening our identification library and allowing actual samples to be identified in spite of shot-to-shot variations. Similarly, known background or confounding spectra may be identified with their own distinct variations and can be rejected.

**Analysis of Conglomerate Aerosols.** Aerosolization of pure mycobacteria mixed with LS or EBC, to simulate infected respiratory fluids, creates a new conglomerate particle type having individual mycobacteria embedded within the background respiratory matrix. TBa-persistent ions are seen in conglomerate sample spectra TBa+EBC and TBa+LS (see Figure 4). For illustrative purposes, only two narrow *m*/*z* regions are depicted, though TBa-persistent ions are seen throughout the spectral range. Guiding

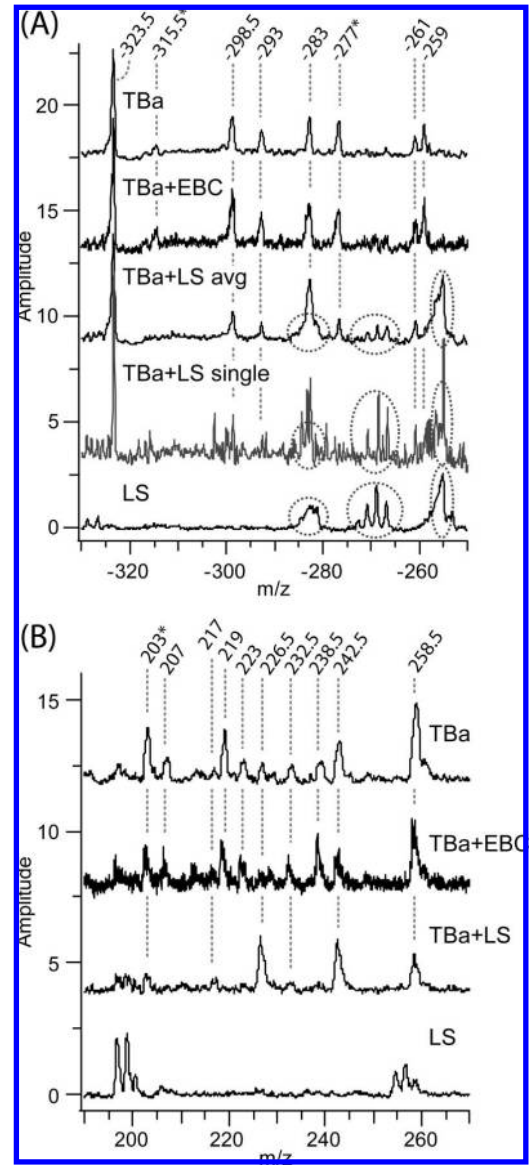


**Figure 4.** Identification of TBa and LS ion signals in conglomerate samples over the *m*/*z* range −330 to −250 (A) and 190 to 270 (B). Spectra are offset and labels rounded to the nearest half-digit for clarity. Guidelines highlight TBa-persistent peaks with *m*/*z* values labeled above the spectra. Asterisks represent peaks that are also observed in spectra from TBa media. Dashed circles in (A) illustrate LS-persistent ion signal in TBa+LS conglomerate particles. A TBa+LS single-particle spectrum is shown (A) to illustrate the conglomerate particle nature of single-particle data.

lines highlight TBa-persistent peaks within the conglomerate spectra, and *m*/*z* values are enumerated (rounded to the nearest half-integer for simplicity). TBa-persistent peaks shown in Figure 4 include the following *m*/*z*: (A) −323.5, −315.5*, −298.5, −293, −283, −277*, −261, and −259, and (B) 203*, 207, 217, 219, 223, 226.5, 232.5, 238.5, 242.5, and 258.5. Dashed circles in Figure 4A show of the persistence of LS peaks in the conglomerate TBa+LS sample.

Figure 4A also shows a single-particle spectrum of TBa+LS in conjunction with the TBa+LS average spectrum. The single-particle spectrum clearly shows the conglomerate nature of the TBa+LS sample on a single-particle basis. A two-component mixed aerosol would be expected to produce a two-component mixed ion signature when the spectra of both distinct particle types are

averaged together. In contrast, a conglomerate aerosol contains single particles that produce a conglomerate ion pattern, not just a simple superposition of the respective ions. The single-particle TBa+LS spectrum (Figure 4A) shows the conglomerate nature of this sample, producing single-particle mass spectra having ion contributions from both TBa and LS simultaneously. Similarly, TBv-infected human sputum samples would contain tuberculosis bacilli interspersed within respiratory fluids. The detection and identification of a simulated pathogen ion pattern within a complicated background ion signal on a single-particle basis is a new and exciting advancement in single particle aerosol mass spectrometry.

**Potential for Bacteria Species Level Identification.** Another challenge for implementing SPAMS as a tuberculosis detection technology in a clinical environment is the possible presence of other nontuberculosis bacteria (NTB). Pulmonary tuberculosis symptoms may arise from nontuberculosis lung infections. To approach the issue of distinguishing tuberculosis from other NTB infections, we compare TBa with MSm.

MSm is a fast-growing nonpathogenic mycobacteria that is widely used as a model organism to study the biology of other virulent and extremely slow-growing species such as *M. tuberculosis*.[21] In this work, we use MSm as a near-neighbor confounder for TBa. Using SPAMS, TBa ion signals can be distinguished from MSm spectra in single-particle data with relatively high accuracy in both pure and, more importantly, conglomerate samples. Data from pure (TBa and MSm) and conglomerate (TBa+EBC, MSm+EBC, TBa+LS, MSm+LS) samples were collected (two selected regions are shown, Figure 5). TBa-persistent peaks shown in Figure 5 include the following $m/z$: (A) −199, −197, −181, −165, and −159 and (B) 115*, 130.5*, 140.5*, 147, 156.5, and 158.5. The largest amplitude TBa-persistent peaks observed over the ±500 $m/z$ region studied are −197, −181, 115*, and 130.5*. Data analysis for this experiment concentrated on TBa ions; however, some MSm ions were observed and two are highlighted (104 and 120 $m/z$) in Figure 5B. The single dashed circle in Figure 5A identifies LS signal in both LS conglomerate spectra. Chemical identities of persistent ions have not yet been fully determined. Many of the persistent peaks have masses consistent with biomarkers recently identified by Phillips et al.,[22] but further experiments would be required to determine definitive molecular identifications.

A patient suspected of pulmonary tuberculosis would present with symptoms similar to any pulmonary infection. The data in Figure 5 reveal how rapid reagentless identification and distinction of tuberculosis infections from other similar bacterial infections may be possible with further research. Thus far, only one comparison has been made, TBa and MSm, but these data show the potential for some species level bacterial identification and differentiation of bacteria embedded in complex respiratory fluids.

**Alarm Algorithm Development and Testing.** Ideally a SPAMS system used for screening would be operated autonomously with an alarm library and algorithm set to identify the presence of TBa and other organisms of interest. Here we describe the first efforts to develop such an algorithm using the surrogate sample set analyzed above. Figure 6 presents results from the pattern matching alarm library designed for these experiments.

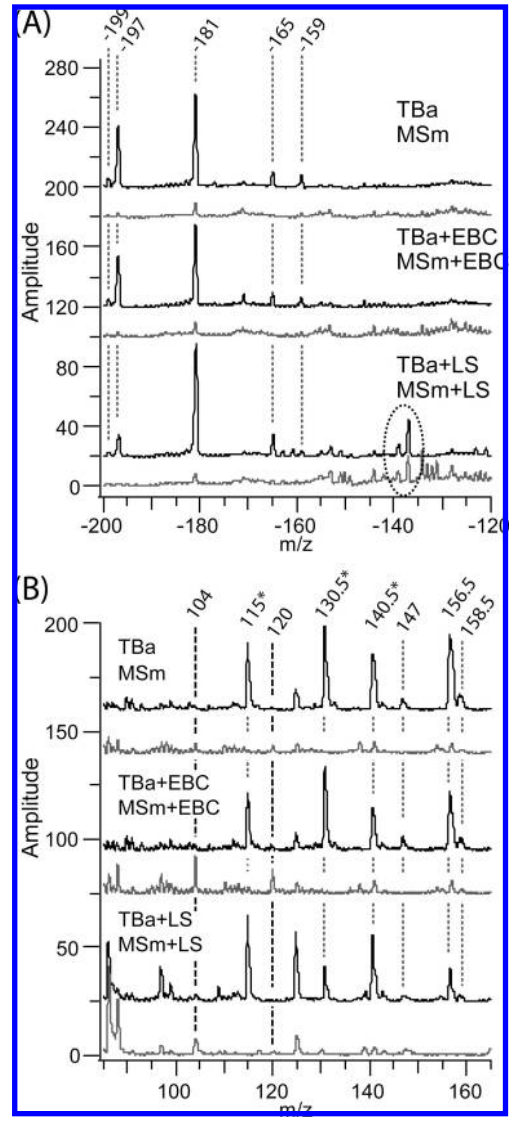


**Figure 5.** Comparison of TBa and MSm ions detected in conglomerate particles over $m/z$ ranges −200 to −120 (A) and 85 to 160 (B). Six spectra are shown: TBa, TBa+EBC, TBa+LS, MSm, MSm+EBC, and MSm+LS. Spectra are offset and labels rounded to the nearest half-digit for clarity. Guidelines highlight TBa-persistent peaks (···) and MSm-persistent peaks (– –) with $m/z$ values labeled above the spectra. Asterisks represent peaks that are also observed in spectra from media. The dashed circle identifies LS-associated ions detected in LS-containing conglomerate particles. Regions shown illustrate the largest amplitude TBa-persistent peaks observed: $m/z$ −197, −181, 115*, and 131.5*.

The pattern matching library was built using TBa, TBa+LS, MSm, MSm+LS, LS, TBa media, and MSm media mass spectral data and optimized for TBa detection. Optimization consisted of removing spectral types in the library that caused excessive cross-identifications within the training sets. With these procedures, TBa can be differentiated from near-neighbor MSm in pure and conglomerate samples. Results shown (Figure 6) are for a test set of 100 randomly selected spectra per sample (where the test set is independent of training set data). Alarm results are tabulated and illustrated by color-coded bar graphs. Boldface numbers in

(21) Vindal, V.; Suma, K.; Ranjan, A. *BMC Genomics* **2007**, *8*, 289.
(22) Phillips, M.; Cataneo, R. N.; Condos, R.; Ring Erickson, G. A.; Greenberg, J.; La Bombardi, V.; Munawar, M. I.; Tietje, O. *Tuberculosis* **2007**, *87*, 44–52.

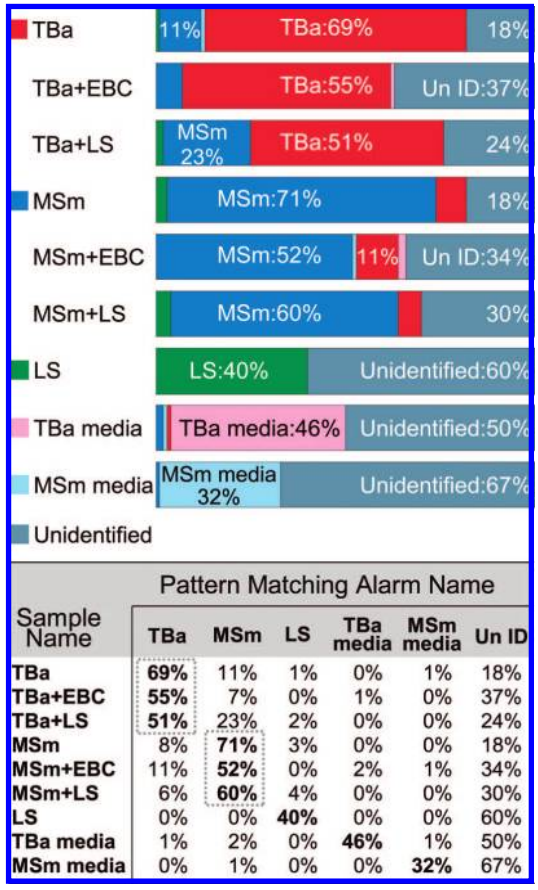


| | Pattern Matching Alarm Name | | | | | |
|---|---|---|---|---|---|---|
| Sample Name | TBa | MSm | LS | TBa media | MSm media | Un ID |
| TBa | **69%** | 11% | 1% | 0% | 1% | 18% |
| TBa+EBC | **55%** | 7% | 0% | 1% | 0% | 37% |
| TBa+LS | **51%** | 23% | 2% | 0% | 0% | 24% |
| MSm | 8% | **71%** | 3% | 0% | 0% | 18% |
| MSm+EBC | 11% | **52%** | 0% | 2% | 1% | 34% |
| MSm+LS | 6% | **60%** | 4% | 0% | 0% | 30% |
| LS | 0% | 0% | **40%** | 0% | 0% | 60% |
| TBa media | 1% | 2% | 0% | **46%** | 1% | 50% |
| MSm media | 0% | 1% | 0% | 0% | **32%** | 67% |

**Figure 6.** Pattern matching alarm algorithm results for a test set of 100 randomly selected particles per sample (where the test set is independent of training set data). The pattern matching library was built using TBa, TBa+LS, MSm, MSm+LS, LS, TBa media, and MSm media mass spectral data and optimized for TBa detection. Results are detailed in table form and illustrated by color-coded bar graphs. Boldface numbers in the table correspond to expected results; i.e., TBa+EBC sample is expected to be frequently identified as TBa.

the Figure 6 table correspond to correct bacterial identification; for example, TBa is correctly identified in the TBa+LS sample for 51% of the particles. In addition to composite effects, a fraction of these particles likely do not contain bacteria and thus a lower identification rate is expected relative to the pure sample. EBC-containing samples were not introduced as part of the algorithm's training set, but alarm results still identify the EBC containing test sets correctly.

TBa is identified in 69−51% of the particles depending on background content. Similar results are seen with MSm, 70−52%. Cross talk between TBa and MSm is seen; with TBa misidentified as MSm 11, 7, and 23% of the time for pure TBa, TBa+EBC, and TBa+LS, respectively. MSm is misidentified as TBa 8, 11, and 6% of the time for pure MSm, MSm+EBC, and MSm+LS samples, respectively. It is unlikely that all single-particle misidentification will ever be eliminated from samples as chemically similar as these two mycobacteria. Nonetheless, by knowing the single-particle misidentification rates for relevant particle types, the false positive diagnosis rate and response time can be optimized. Thus, with a known TBa misidentification rate, a multiple particle sample, and fast analysis, high-confidence, rapid TBa detection is possible with a low false alarm rate. For example, given a sample of 100 particles and an alarm threshold of >23 particles, TBa can be identified in a background of MSm with a false positive rate of less than $10^{-5}$ according to binomial statistics.

One challenge in building the alarm library was eliminating spectral types showing features characteristic of growth media from the mycobacterial ion signatures. Because the mycobacteria were grown in media, they inherently incorporate the media as part of their chemistry, and thus not all media are readily removed from the mycobacterial samples upon washing. If spectral types consistent with growth media contributions are retained in the TBa library, for example, excessive cross-identifications of TBa with TBa media result. Their removal from the TBa library however reduces the algorithm's overall sensitivity and mycobacterial identification rate. Since artificial growth medium is not present in human samples, improvements to the library, and thus mycobacterial identification rate, could be made given better bacteria purification or human samples.

**Proposed Model for SPAMS Diagnostics in a Clinical Setting.** The results detailed in this paper provide evidence that SPAMS may be useful in quickly screening for tuberculosis in clinical environments. Additional experiments are needed, including progressively more realistic sputum surrogates leading to TBv-containing sputum samples and a broader range of confounder bacterial samples, but it is prudent even now to consider how SPAMS may eventually be used. A proposed scenario for deploying SPAMS in a clinical environment is shown in Figure 1, where the SPAMS system would monitor clinical samples for tuberculosis and give near real-time responses. Two sampling scenarios are proposed: general room air monitoring and aerosolized patient effluent analysis. In the first scenario, the SPAMS system would monitor room air for aerosol particles containing tuberculosis bacteria to study the level of airborne tubercle bacilli produced from tuberculosis patients breathing, talking, and coughing. This air monitoring system would assist in understanding the air safety level and validating the efficacy of facility engineering controls where airborne tuberculosis is prevalent or feared: immigration facilities and transit centers, as well as tuberculosis clinics. In the second scenario, rapid patient screening for tuberculosis may be possible by reaerosolizing a diluted patient sputum sample as shown in Figure 1 or conceivably by direct breath interface.

## CONCLUSIONS

We have expanded the application of SPAMS to the detection of airborne tuberculosis for room air monitoring[12] and performed the first proof-of-concept experiments for applying SPAMS to the detection of sputum sample analysis. The detection and identification of tuberculosis H37Ra embedded in respiratory effluents and discrimination from another mycobacterium is shown. This identification on a single-particle basis is a new and exciting advancement in single-particle aerosol mass spectrometry. Naturally the current results from the proof-of-concept experiments described here do not directly translate to detection of tuberculosis in humans. Many challenges still exist in realizing rapid TBv detection in clinical settings. Patterns for realistic samples must be investigated including virulent tuberculosis, human sputum, TBv confounders, near-neighbor bacteria, and TBv natural muta-

tions. Patient-to-patient sample variations in background lung matrix (sputum) and natural TBv variations must be examined, as these natural changes may greatly affect detection capabilities. The TBv limit of detection and threshold levels must be addressed especially considering that human sputum samples are expected to contain many fewer bacteria per milliliter than the samples used in this study. The number of tubercle bacilli found in patient samples varies widely, but can range from 100 000 acid-fast bacilli per milliliter sputum detectable by microscopy[23] to just hundreds of bacilli detectable by culture and PCR.[24] Future efforts will be directed toward addressing these issues, as well as investigating possible clinical applications and developing a human sample interface. If successful, the SPAMS technique could present unique advantages over current tuberculosis screening methods primarily because it offers rapid and reagentless detection. One day this or similar techniques may reduce hospital costs and perhaps save lives.

(23) Hobby, G. L.; Holman, A. P.; Iseman, M. D.; Jones, J. M. *Antimicrob. Agents Chemother.* **1973**, *4*, 94–104.
(24) Thomson, L. M.; Traore, H.; Yesilkaya, H.; Doig, C.; Steingrimsdottir, H.; Garcia, L.; Forbes, K. J. *J. Microbiol. Methods* **2005**, *63*, 95–98.

## ACKNOWLEDGMENT

The authors thank M.P. Schaefer at CDC/NIOSH for donating the *M. tuberculosis* H37Ra strain and Abbott Laboratories for the Survanta bovine lung surfactant used in this study. The authors greatly appreciate the LLNL Laboratory-Directed Research and Development (LDRD) Program that supported this work under project 05-ERD-053. N.M.S. and A.N.M. performed this research while on appointment as U.S. Department of Homeland Security (DHS) Fellows under the DHS Scholarship and Fellowship Program, administered by the Oak Ridge Institute for Science and Education (ORISE) for DHS through an interagency agreement with DOE. ORISE is managed by Oak Ridge Associated Universities under DOE Contract DE-AC05-06OR23100. This work was performed under the auspices of the U.S. Department of Energy by Lawrence Livermore National Laboratory in part under Contract W-7405-Eng-48 and in part under Contract DE-AC52-07NA27344.

Received for review February 8, 2008. Accepted April 23, 2008.

AC8002825